Investigating the Tooth Contact Based on a High-speed Thermography Monitoring Conducted Under High-reduction Hypoid Gears Meshing Conditions

Kouki Watanabe*, Toshiki Hirogaki, and Eiichi Aoyama

Abstract—Currently, improving the Noise Vibration Harshness (NVH) characteristics of systems is among the most important issues for meeting user needs in the automotive industry. Remember that the tooth surface accuracy significantly influences the vibrations in gear meshing. The hypoid gear used in the automobile differential has a complex shape; hence, estimating its contact conditions is difficult. Therefore, we aim to develop a novel method to analyze the tooth contact conditions by using highly sensitive infrared thermography measurements with a high response. The proposed method acts as a noncontact analysis that is based on monitoring the temperature distribution during meshing between the pinion and gear surfaces. In this report, we designed three hypoid gear types with high-reduction ratios. Subsequently, a tooth contact analysis was carried out using thermography measurements. As a result, the relationship between the temperature rise at the tooth contact area was clarified.

Index Terms—High-reduction, hypoid gear, thermography, gear mesh loss

I. INTRODUCTION

Gears are used under severe conditions and often utilized in applications that require high speeds and load torques. Under such conditions, the tooth surface can be damaged owing to scoring. To develop a countermeasure against scoring, researchers have focused on various parameters such as the type of lubricant, material, and tooth profile. However, because the instantaneous temperature of the tooth surface significantly affects the scoring load, it is necessary to consider the scoring limit value. Methods that consider the tooth surface temperature as a single index have attracted considerable attention [1].

Recently, advances in infrared sensors and sensor output signal processing technology have improved the spatial resolution of temperature measurements. Consequently, the so-called infrared thermography that is capable of real-time and high-response measurements has been developed [2]. Based on the developments in the infrared image measurement technology, previous research has used infrared thermography technology to evaluate the meshing state of the hypoid gears during driving and developed a novel tooth contact monitoring method [3].

In these studies, the rise in the contact surface temperature during driving was acquired using thermography. Subsequently, the contact state was estimated by analyzing the temperature distribution. Hypoid gear pairs are widely used as the final reduction gear for automobiles because of the following advantages: they can be installed more securely than general spiral bevel gear pairs, the shaft diameter can be increased by increasing the torsion angle of the pinion gear, they have a higher reduction ratio than that of bevel gear pairs, and they mechanical reduce noise [4].

Furthermore, recently, regulating CO_2 automobile emissions in response to global warming through various policies and risk of fossil fuel depletion have become global issues. Subsequently, efforts to electrify automobiles and increase their fuel efficiency are gaining momentum. Accordingly, electrical motors must be smaller, lighter, and more power-efficient, leading to improved fuel economy; thus, more efficient reduction gears, capable of higher reduction speeds are required [5-11]. Although there have been several studies that examine design methods to realize high-reduction-ratio hypoid gears, few studies have investigated the drive and meshing conditions of gear pairs with high reduction ratios [12-14].

In this study, we examined the versatility of the temperature analysis method proposed here, as well as the relationship between meshing efficiency and temperature rise in various gear pairs, using gear pairs with different reduction ratios, especially in the high-reduction region using the experimental gears. As a result, monitoring the tooth surface temperature by thermography was proven useful for gears with different reduction ratios.

II. EXPERIMENTAL DEVICES

A. Gear Driving Device

An ATM-460 (Kokusai Co., Ltd.), which measures the meshing transmission error, was used during the driving experiments. The maximum load torque was 100 Nm for the driven gear, while the maximum rotational speed of the drive gear was 60 min^{-1}.

B. Device Used for Middle-infrared Imagery

An SC7000 (FLIR Systems, Inc.) mid-infrared thermograph was used to measure the temperature distribution. This thermograph cools indium antimonide (InSb) infrared rays by detecting the elements with a Stirling air conditioner and achieves highly sensitive and precise temperature detection. In addition, the thermograph could be configured to detect temperatures as low as 0.02 °C.

C. Lubrication

Differential oil (GL-5, 80W-90, Nissan Motor Co., Ltd.) was applied to the tooth surfaces using a brush, on both the pinion and gear.

D. Specifications of Hypoid Gear Pairs

Three types of Gleason hypoid gear pairs with different reduction ratios were considered. Fig. 1 shows the high-reduction hypoid gear pairs with different reduction ratios. In this study, to focus on the reduction ratio effect, other specifications were kept equal as much as possible. Here, we consider that more than 10 reduction is high reduction ratios, as shown in Fig. 1 (A) and (B).
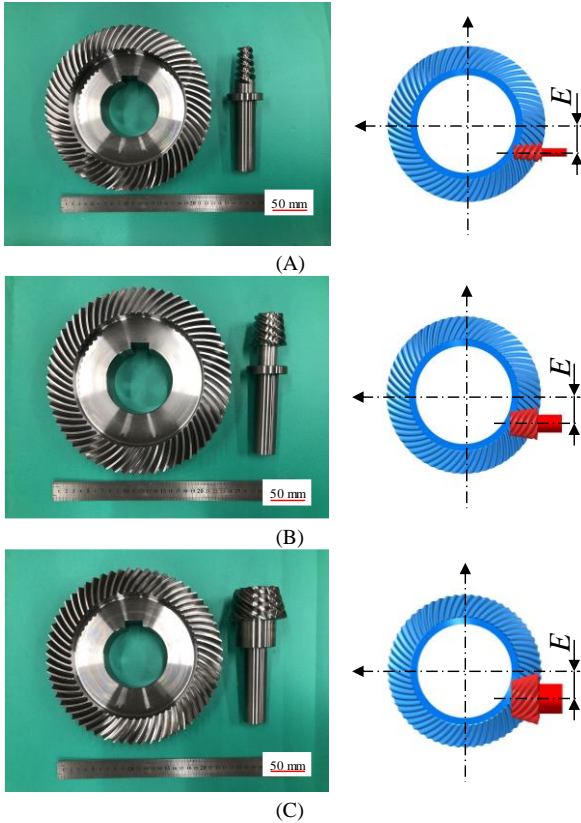

(A)

(B)

(C)

Fig. 1(a). Reduction ratio 3/60; (b) Reduction ratio 6/60; (c) Reduction ratio 12/60. High reduction hypoid gears with different reduction ratios.

III. EXPERIMENTAL AND ANALYSIS METHODS

A. Measurement of Tooth Surface Temperature

To observe the rotating gear, an infrared camera was attached to a tripod and installed as shown in Fig. 2. In this study, the rotation direction refers to the direction in which the convex tooth surface of the pinion meshes with the gear-side concave tooth surface. The pinion was rotated while the driving device applied a load, and the situation was captured using thermography. The frame rate of the camera was set to (pinion rotation speed n) × 2.5 Hz, with an integration time of 2 ms ensure continuous shooting.

The thermography conditions were set based on the FLIR Altair software used for thermography. The emissivity was proofread using a black body tape (emissivity 0.94); the emissivity for the experiment was determined as 0.39. In addition, an extraction line was defined in the obtained thermal images, shown in Fig. 3. This line was at the same position in all frames. Consequently, it was possible to obtain temperature data immediately after meshing [15]. Table I lists the experimental conditions used to obtain tooth surface temperature measurements. An experiment under each condition was conducted only once, and the experimental data logged on the same day were compared to eliminate external factors.
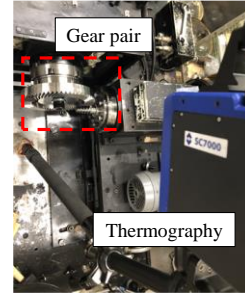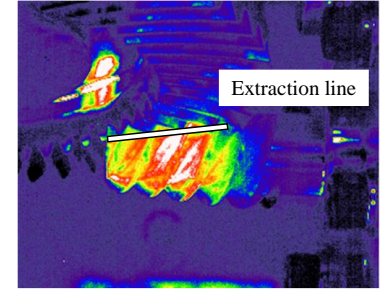

Fig. 2. Experimental setup.　　Fig. 3. Extraction line on thermal image.

TABLE I: EXPERIMENTAL CONDITIONS

Rotation speed [min⁻¹]	20, 40, 60
Load torque [Nm]	20, 60, 100
Exposure time [s]	30

B. Device Used for Middle-infrared Imagery

Focusing on the temperature profile of the sampling line defined in Fig. 3, a continuous temperature profile can be obtained via a frame-by-frame image transmission. By connecting the continuous profiles to create an isotherm graph, a temperature distribution diagram was created, in which the cooling time after meshing was almost constant. Fig. 4 illustrates this process. Here, the exposure time was set to 2 ms.
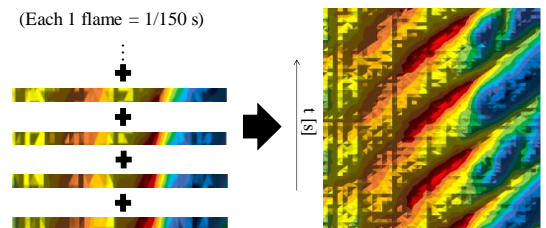

Fig. 4. Temperature distribution map.

IV. RESULTS AND DISCUSSION

A. Tooth Surface Temperature

Fig. 5 shows an example of the average temperature on the sampling line obtained using the method depicted in Fig. 3. For a hypoid gear used in a previous study, change in the temperature after 30 s was defined as a temperature increase, taking the lowest temperature in the graph as the reference.

However, for the gear pair with the high reduction ratio targeted in this study, the defined sampling line does not reliably capture the tooth surface temperature transition because of the large torsional angle of the pinion. To further discuss the acquired temperature measurements, a temperature data distribution map was created using the method demonstrated in Fig. 4. Fig. 6 shows the tooth surface temperature distribution diagram for a high-reduction hypoid

gear with a tooth ratio of 3/60, pinion speed of 60 min^{-1}, and gear load torque of 100 Nm. Fig. 7 shows a thermal image of the temperature data and temperature distribution created from the data in the same image. From these figures, notice that the area of temperature increase is divided into two parts, the tooth surface and tooth tip, when each tooth is separated into two parts. Furthermore, the defined sampling line captures multiple teeth simultaneously and includes the temperature of the tooth tips. Therefore, it is necessary to reconsider the average value calculation method for these temperature measurements. Therefore, the tip temperature of one tooth in the tooth surface temperature distribution was removed; only the tooth surface was extracted to obtain the average temperature of the entire tooth surface to capture the pure temperature rise of the tooth surface owing to meshing. The temperature increase was defined as the difference between the average tooth surface temperatures after the drive stabilized and after 30 s. The results regarding the temperature rise values calculated using this method are summarized for each condition in Fig. 8. Fig. 8(a) and 8(b) depict the temperature rise as a function of changes in load torque and rotation speed conditions when the pinion speed is fixed at 60 min^{-1} with 100 Nm of gear-side load torque. Fig. 8 shows that the temperature rise values for all conditions are lower than the average temperature rise on the sampling line obtained by the conventional method. The temperature rise increases linearly with increasing load torque and logarithmically with increasing rotation speed, which is consistent with the trend described in previous studies.
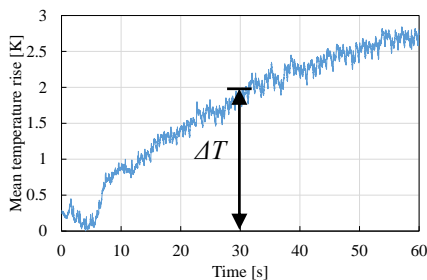

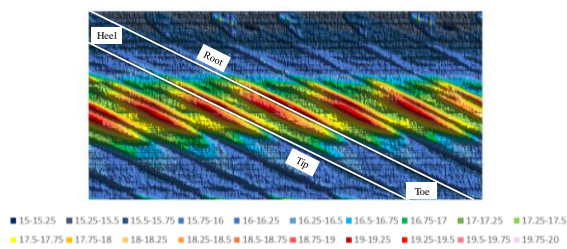Fig. 5. Mean temperature rise on the exaction line (ratio 3/60, 60 min^{-1}, 100Nm).

Fig. 6. Tooth temperature distribution diagram.
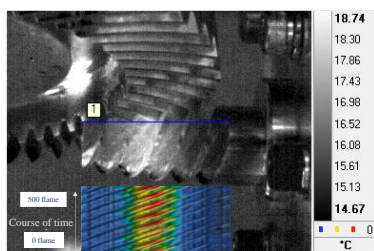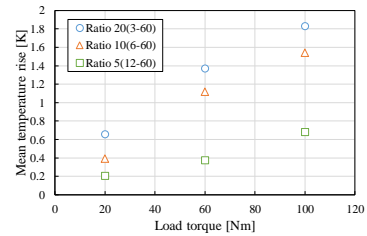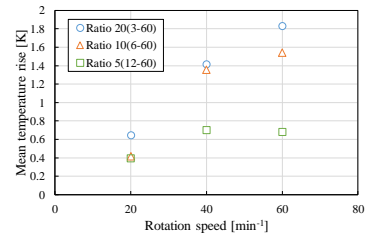

Fig. 7. Comparison of a thermal image and tooth surface temperature distribution chart.

(a)

(b)

Fig. 8. Comparison of mean temperature rise on tooth surface. (a) Relationship between the load torque and temperature rise (Rotation speed 60 min^{-1}); (b) Relationship between rotation speed and temperature rise (Load torque 100 Nm)

B. Relationship Between Gear Pair Engagement Loss and Tooth Surface Temperature Rise

Fig. 8 shows that different reduction ratios of gear pairs cause differences in temperature rise of up to 300 %, even under the same load torque and speed conditions. For the gears used during the experiments, we considered that differences in the twist angle, pinion diameter, number of teeth, and other factors that cannot be avoided by design owing to changes in the reduction-ratio are caused the temperature change on the tooth flanks. First, to capture the change in temperature rise as a function of reduction ratio, the results presented in Fig. 8 are reorganized in Fig. 9 with the reduction-ratio on the horizontal axis. These figures demonstrate that the temperature rise increases logarithmically with an increase in the reduction ratio for each condition. In a previous study, the temperature rise trend variation with respect to offset variations for three types of gears with different offsets was clarified; however, in general, the transmission efficiency of a gear pair decreases as the offset increases. This means that losses indeed occur, which are converted to frictional heat during the meshing contact. Therefore, the relationship between the meshing efficiency (loss) of each gear pair and temperature rise was discussed in this study [16][17]. The high-reduction hypoid gears used in this study are also considered to have a significant change in the pinion torsion angle, as well as the other factors that affect transmission efficiency owing to differences in reduction ratios. Therefore, a comparison was made between the mesh efficiency (loss) and temperature rise of each gear pair for six gear pair types, including the three hypoid gear types with different offsets described in a previous study in addition to the three high-reduction hypoid gears depicted in this study. The temperature rise was defined as the average temperature rise of the pinion side tooth surface over 30 s when driven at 60 min^{-1} and 100 Nm for all gear pairs. Moreover, the transmission efficiency of the gears was calculated using KIMoS, a spiral bevel gear calculation software provided by KLINGELN BERG (Table Ⅱ). Fig. 10 shows the results for each gear type, with the loss due to meshing on the horizontal

axis and temperature rise value on the vertical axis.

Fig. 10 demonstrates the trend of the logarithmic temperature rise versus loss for each gear type. However, the temperature rise values for high-reduction hypoid gear pairs were smaller than those for the gear pairs used in a previous study. Because the different design specifications of each gear pair significantly influence the temperature rise, we will discuss the temperature rise considering the differences in the specifications. The main differences in specifications that may cause a temperature rise are the gear diameter and pinion tooth geometry. The gear drive used in this study applies torque by controlling the speed of the driven side. For the same torque value, the gear diameter determines the total load applied to the tooth flanks. In addition, among the high-reduction hypoid gears, the pinion teeth with a reduction ratio of 3/60 have fewer teeth and a shape with a larger torsional angle. Consequently, the tooth area subjected to load varies greatly from gear pair to gear pair. Therefore, equation (1), which considers the surface pressure of each gear pair, is used to evaluate the relationship; where ΔT_x [K] is the temperature rise of the tooth surface and P_x [N/mm^2] is the surface pressure obtained by dividing the tooth surface load F [N], which is obtained by dividing the torque T [Nm] by the gear-side pitch circle radius r [m], by the tooth area S [mm^2], defined as the product of the tooth trace length b_ℓ [mm] and tooth height h_e [mm].

$$k = \Delta T_x / P_x \qquad (1)$$

TABLE II: Percentage Meshing Loss

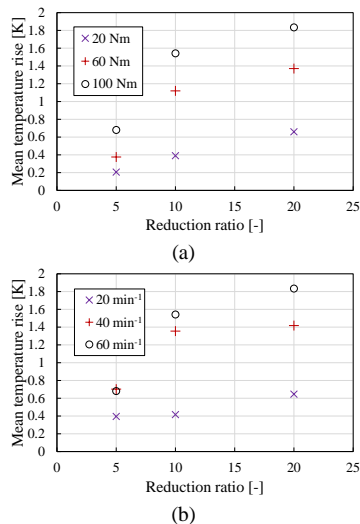|	Hypoid		
Offset [mm]	0	10	20
Gear mesh loss [%]	2.46	4.31	5.51
	High-reduction hypoid		
Reduction ratio [-]	5	10	20
Gear mesh loss [%]	6.49	17.35	24.76

(a)

(b)

Fig. 9. Comparison of mean temperature rise owing to differences in reduction ratio. (a) Relationship between the reduction ratio and temperature rise (Rotation speed 60 min^{-1}); (b) Relationship between the reduction ratio and temperature rise(Load torque 100 Nm)
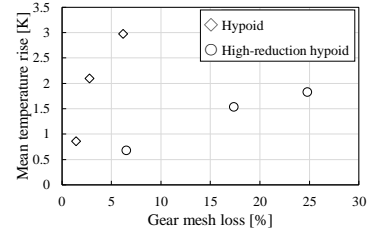

Fig. 10. Relationship between the gear mesh loss and temperature rise.

V. Conclusion

In this study, a thermal image of the tooth surface was obtained using high-speed video infrared thermography to examine the driving tooth surface used in hypoid gears with different reduction ratios. The following conclusions were drawn:

1) The temperature rise in the tooth flanks of high-reduction hypoid gears with high reduction ratios can be obtained using a temperature analysis method with a thermal imaging camera suggested in this study. Moreover, we clarified that the temperature rise changes logarithmically with the reduction ratio.

2) Temperature rise evaluation methods were devised for hypoid gear pairs with different specifications, and the correlation between engagement loss and temperature rise was accurately demonstrated.

Conflict of Interest

The authors declare no conflict of interest.

Author Contributions

Kouki Watanabe conducted the research, analyzed the data, and wrote the paper. Toshiki Hirogaki and Eiichi Aoyama helped write the paper; all authors had approved the final version.

References

[1] Y. Terauchi, "Measurement of tooth surface temperature of gear," *Journal of Precision Machinery*, vol. 36, no. 1, 1970, pp. 34–41.

[2] T. Sakagami, "Recent progresses in thermoelastic stress measurement by infrared thermography," *Journal of Experimental Mechanics*, vol. 1, no. 3, 2001.

[3] T. Hirogaki, E. Aoyama, R. Pihet, and K. Niwa, "Investigation of temperature hysteresis on tooth contact surface of hypoid gears using middle-infrared ray imagery," *Journal of Advanced Mechanical Design, Systems, and Manufacturing*, vol. 8, no. 3, 2014).

[4] C. Naruse, "Gear basics and design," 1988, pp. 50–61.

[5] M. Kaizuka, T. Tachibana, T. Kosaka, S. Doki, and Y. Ota, "Latest technological trends for electrification of automobile technologies," *IEEJ Transactions on Industry Applications*, vol. 139, no. 6, 2019.

[6] T. Tokizaki *et al.*, "Development of single tooth pinion gear to achieve high efficiency and high speed reduction, transactions of society of automotive engineers of Japan," vol. 51, no. 1, 2020.

[7] H. and J. Stadtfeld, *Automotive Drive Concepts*, Company Publication, The Gleason Works, 2008, pp.1–8.

[8] Hermann and J. Stadtfeld, "Tribology aspects in angular transmission systems," *Part VIII*., Super-Reduction Hypoid Gears, pp. 42–48, 2008.

[9] M. Mohammadpour, S. Theodossiades, H. Rahnejat, and P. Kelly, "Transmission efficiency and noise, vibration and harshness refinement of differential hypoid gear pairs," vol. 228, no. 1, 2014.

[10] L. Arthur and S. E. Wildhaber, "Design, production and application OF the hypoid rear-axle gear," *SAE Transactions*, vol. 21, 1926.

[11] M. G. Donley, T. C. Lim, and G. C. Steyer, "Dynamic analysis of automotive gearing systems," *SAE Technical Paper*, no. 920762, 1992.

[12] A. Suzuki,. L. Tarutani, and T. Aoyama, "Design of high-reduction hypoid gears meshing in plane of action," *Journal of Advanced Mechanical Design, Systems, and Manufacturing*, vol. 11, no. 6, 2017.

[13] N. Ito and K. Takahashi, "Design of high-reduction hypoid gears (1st report, fundamental relationships for designing by pinion shapes)," *Transactions of the Japan Society of Mechanical Engineers*, vol. 57, no. 536, 1991.

[14] N. Ito and K. Takahashi, "Design of high-reduction hypoid gears (2nd report, method for designing by gear spiral angle parameter)," *Transactions of the Japan Society of Mechanical Engineers*, vol. 57, no. 537, 1991.

[15] K. Mukaiyama, S. Arao, S. Matsui, M. Nakagawa, T. Hirogaki, and E. Aoyama, "Investigation of meshing phenomenon of hypoid gears with different offsets via high response infrared video thermography," *Forschung im Ingenieurwesen*, vol. 83, 2019.

[16] M. Kolivand, S. Li, and A. Kahraman, "Prediction of mechanical gear mesh efficiency of hypoid gear pairs," *Mechanism and Machine Theory*, vol. 45, 2010.

[17] H. Xu and A. Kahraman, "Prediction of friction-related power losses of hypoid gear pairs," in *Proc. Institution of Mechanical Engineers, Part K: J. Multi-body Dynamics*, vol. 221, 2007, pp. 387–400.